STUDIA INFORMATICA 2003
Volume 24 Number 4 (56)

Katarzyna STĄPOR, Lesław PAWLACZYK,
Politechnika Śląska, Instytut Informatyki
Marek RZENDKOWSKI
Szpital Wielospecjalistyczny, Oddział Okulistyczny - Gliwice

ADAPTIVE LOCAL THRESHOLDING FOR AUTOMATIC SEGMENTATION OF EYE-CUP IN FUNDUS EYE IMAGES

Summary. In this paper a new algorithm of the eye cup segmentation from fundus eye images (fei) is proposed. It is based on an adaptive local thresholding technique performed on a channel a* of a L*a*b* color model. The obtained contour of eye-cup region will be used in a classification procedure supporting ophthalmologist in glaucoma diagnosing.

Keywords: image segmentation, adaptive thresholding, glaucoma

LOKALNE ADAPTACYJNE PROGOWANIE W AUTOMATYCZNEJ SEGMENTACJI WNĘKI NACZYNIOWEJ NA CYFROWYCH OBRAZACH DNA OKA

Streszczenie. W artykule tym przedstawiono nowy algorytm segmentacji wnęki naczyniowej na podstawie obrazów dna oka pozyskanych z funduskamery. W algorytmie zastosowano metodę adaptacyjnego, lokalnego progowania składowej a* modelu kolorów L*a*b*. Uzyskany kontur wnęki naczyniowej może zostać użyty w procedurze klasyfikacji, która ma wspomagać okulistę w diagnozowaniu jaskry.

Słowa kluczowe: segmentacja obrazu, progowanie adaptacyjne, jaskra

1. Introduction

Glaucoma is a group of diseases characterized by the proceeding optic nerve neuropathy, which leads to the rising diminution in vision field, ending with blindness. The correct eye disk contains *neuroretinal rim* of pink color placed on the *eye disk* circuit and centrally placed

yellowish *eye cup* (Fig. 3). Glaucomatous changes in retina appearance embrace various changes in neuroretinal rim and eye cup, as the result of nerve fibers damages.

Examination of the eye disk structures is one of the most important in glaucoma diagnosis. Searching for glaucoma damages during routine examination (i.e. based on ophthalmoscope and slit lamp with Volk lens) is not an easy task and gives uncertain results even with the experienced ophthalmologist. There is a need for objective methods of automatic eye disc structures localisation.

In the existing approaches to automatic segmentation of fei for supporting glaucoma examinations [1,3,7,9,10] researchers focused on the detection of the eye disk and its characteristics. Typical methods of finding eye disk boundary are: active contour model (snakes), arc fitting to eye disk boundary using error minimization. In [5] important proofs that shape of the eye cup and its numerical characteristics correlate with progress of glaucoma disease were presented.

In this paper the new automatic segmentation method of the eye cup from fundus eye images is presented. The novelty relies on the automatic segmentation of the eye cup from fundus eye images, which wasn't the area of interest in the past. Fig. 1 shows the steps of the proposed eye cup segmentation algorithm. The next step will be a classification of digital fundus eye images (**fei**) into normal and glaucomatous ones based on the suitable shape descriptors, which is a subject of our current work.

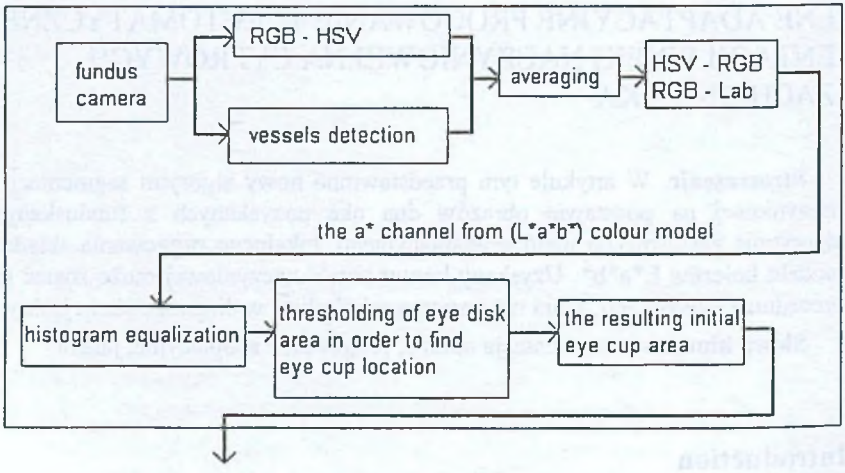

Fig. 1. Stages of the eye cup segmentation method
Rys. 1. Etapy segmentacji wnęki naczyniowej

2. The method

Before the algorithm starts a user is asked to indicate a rectangle, which contains eye disk, to decrease the computation time.

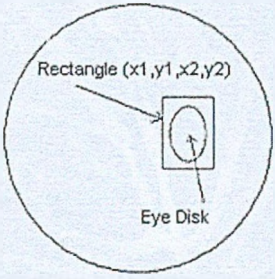

Fig. 2. Rectangle specified by user containing eye disk
Rys. 2. Prostokąt wskazany przez użytkownika zawierający dysk optyczny

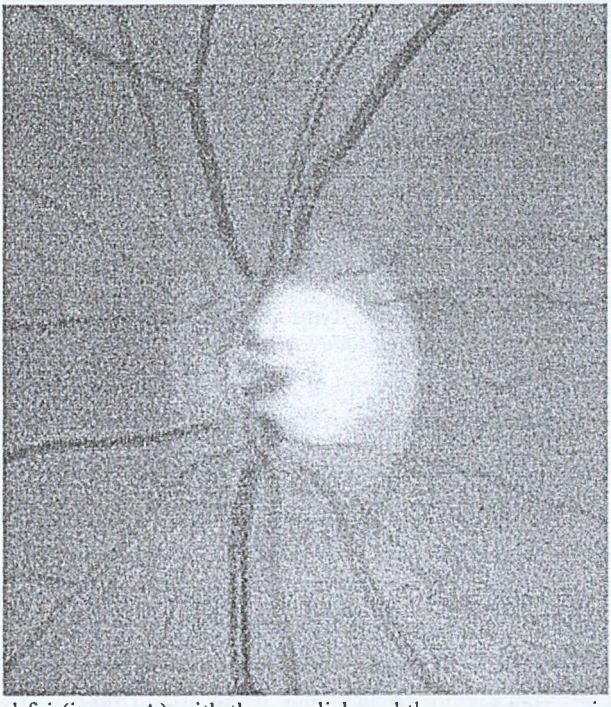

Fig. 3. The initial fei (image A) with the eye disk and the eye cup area in the central part
Rys. 3. Wstępna postać obrazu (obraz A) z widocznym dyskiem optycznym oraz wnęką naczyniową w centralnej części

2.1. Vessels averaging

The algorithm for vessels averaging is based on the method of vessels detection described in [1]. The example of image with the detected vessels is shown in Fig. 4.

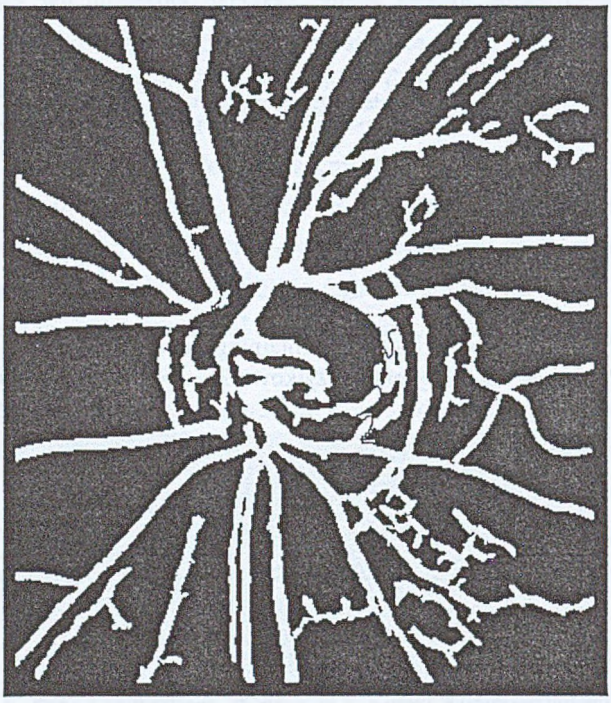

Fig. 4. Image A with the detected vessels
Rys. 4. Obraz A z wykrytymi naczyniami krwionośnymi

All white pixels (i.e. pixels comprising vessels) lying inside the user rectangle belong to the subregion named here $R_{eyecup-vessels}$. First, the input image is converted form RGB to HSV color model [2,4]. By overlaying the image with detected vessels on the input, converted image all border pixels of the detected vessels are found (subregion $R_{eyecup-vessels}$). For each border pixel in $R_{eyecup-vessels}$ its new color components $[H_{avg}, S_{avg}, V_{avg}]$, being the average of the appropriate components of pixels lying in the 8-connected neighborhood outside of $R_{eyecup-vessels}$ region are found. After recalculation of all border pixels, they are deleted, new border pixels are found and the process is repeated until size of $R_{eyecup-vessels}$ is higher than 0.

Fig. 5. Averaging vessels in the eye disk area from image A
Rys. 5. Uśrednianie naczyń krwionośnych w obrębie dysku optycznego na obrazie A

2.2. Image color model conversions

Color is perceived by humans as a combination of three primary colors: R (red), G (green) and B (blue). From R, G, B representation we can derive other kinds of color representations (spaces) by using either linear or non-linear transformations.

Two color spaces are used in the presented segmentation algorithm: *HSV* and (L*,a*,b*) [2].

HSV color space is composed of three channels: *H* (Hue) represents basic colors, *S* (Saturation) is a measure of a purity of a color and *V* (Value) is a measure of intensity. Color information is represented by hue and saturation values, while intensity, which describes the brightness of an image is represented by value component. There are algorithms for transformation RGB into HSV coordinates [4].

The main goal was to find a proper color model, which could distinguish the eye cup from the rest of fei. During examinations of different color models, *L*a*b** color space was the best for this purpose. It can be derived through CIE XYZ color space from RGB model.

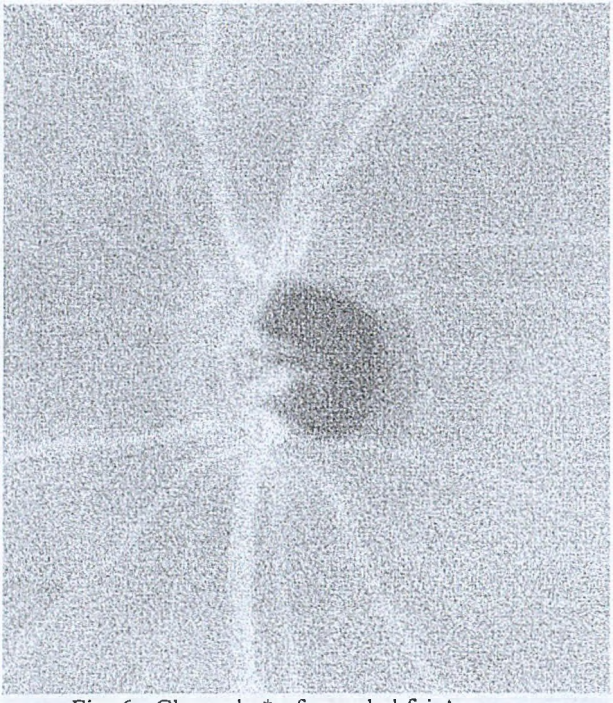

Fig. 6. Channel a* of sampled fei A
Rys. 6. Kanał a* przykładowego obrazu A

CIE (Commission Internationale de l'Eclairage) [2,4] color model has three primaries denoted as X,Y,Z. Any color can be specified by the combination of X,Y,Z. The values of X,Y,Z can be computed by a linear transformation from RGB tristimulus coordinates.

$$\begin{bmatrix} X \\ Y \\ Z \end{bmatrix} = \begin{bmatrix} 0.607 & 0.174 & 0.200 \\ 0.299 & 0.587 & 0.114 \\ 0.000 & 0.066 & 1.116 \end{bmatrix} \begin{bmatrix} R \\ G \\ B \end{bmatrix}$$

The *(L*,a, *b*)* model can be computed as follows:

$$L^* = 116\left(\sqrt[3]{\frac{Y}{Y_o}}\right) - 16$$

$$a^* = 500\left[\sqrt[3]{\frac{X}{X_o}} - \sqrt[3]{\frac{Y}{Y_o}}\right]$$

$$b^* = 200\left[\sqrt[3]{\frac{Y}{Y_o}} - \sqrt[3]{\frac{Z}{Z_o}}\right]$$

$Y/Y_0 > 0.01, X/X_0 > 0.01, Z/Z_0 > 0.01$, and (X_0, Y_0, Z_0) are (X, Y, Z) values for standard white. In Figs. 6, 7 channels a^* and b^* of a sampled fei A are shown.

It's evident, that the best for further examinations is the channel a^*. It's observable, that the eye cup appears as a dark part and is the only element in the image with such a low luminance.

Fig. 7. Channel b* of sampled fei A
Rys. 7. Kanał b* przykładowego obrazu A

2.3. Histogram equalization

Let $r_1, \ldots, r_L$ (L define number of all levels) define the intensity values (color) in the image. The histogram create a set of values: $p(r_1), \ldots, p(r_L)$ evaluated by formula:

$$p(r_j) = n_j/n$$

where n_j is the number of pixels in image characterized by intensity level r_j and n is the number of all pixels in image.

The histogram equalization transformation [4] is given by the function:

$$s_k = T(r_k) = \sum_{j=1}^{k} p(r_j),\ k=1,2,\ldots,L$$

The result of using this transformation is a histogram much more equalized, which uses the whole set of intensity levels.

The operation of histogram equalization is executed on the a^* component of a $L^*a^*b^*$ model (Fig 6) to improve the image contrast.

2.4. Image thresholding

Thresholding provides a way to separate out the regions of the image corresponding to objects in which we are interested, from the regions of the image that correspond to background. It is an operation, that involves tests against a function T of the form [4]:

$$T = T[x,y,p(x,y),f(x,y)]$$

where f(x,y) is the gray level of point (x,y) and p(x,y) denotes some local property of this point – for example the average gray level of a neighborhood centered at (x,y). A thresholded image g(x,y) is created by defining:

$$g(x,y) = \begin{cases} 0 & f(x,y) \le T \\ 1 & f(x,y) > T \end{cases},$$

where T is a threshold. When T depends only on $f(x,y)$, the threshold is called global. In adaptive thresholding, for each pixel in an image, a threshold has to be calculated. Adaptive methods are particularly useful in the cases, where there is a large range of variation in gray scale from one part of the image to another, so that a single fixed threshold cannot be used for the entire image. There are two main approaches to finding a local threshold [4]:

1) Dynamic thresholding

Finding a local threshold by statistically examining the intensity values of a local neighborhood of each pixel. The statistic, which is most appropriate, depends largely on the input image.

2) Local thresholding

Divides an image into an array of subimages and then finds the optimum threshold for each subimage by investigating its histogram. The threshold for each single pixel is found by interpolating the results of the subimages.

The resulted image (i.e. channel a^*) with the equalized histogram is a subject of the proposed adaptive local thresholding method. The method (based on variable thresholding described in [8]) is composed of the following stages:

1. The image is divided into windows.
2. A histogram $F(i)$ for i=0,...,255 is computed for each window.

3. A least square fit of :

$$f(i) = \frac{P_1}{\sigma_1} e^{-(i-\mu_1)^2/2\sigma_1^2} + \frac{P_2}{\sigma_2} e^{-(i-\mu_2)^2/2\sigma_2^2}$$

the histogram *F(i)* is found by adjusting the parameters $P_1, P_2, \sigma_1, \sigma_2, \mu_1, \mu_2$. This is done as follows. The histogram is smoothed by taking a local weighted average. On the smoothed histogram the deepest valley *v* is found and is used to divide the histogram into two parts. Initial estimates of the parameters are computed on these two parts:

$$N_1 = \sum_{i=0}^{v} F(i)$$

$$N_2 = \sum_{i=v}^{255} F(i)$$

$$\mu_1 = \frac{1}{N_1} \sum_{i=0}^{v} F(i) * i$$

$$\mu_2 = \frac{1}{N_2} \sum_{i=v}^{255} F(i) * i$$

$$\sigma_1 = \sqrt{\frac{1}{N_1} \sum_{i=0}^{v} F(i) * (i-\mu_1)^2}$$

$$\sigma_2 = \sqrt{\frac{1}{N_2} \sum_{i=v}^{255} F(i) * (i-\mu_2)^2}$$

$$P_1 = \frac{N_1 \sigma_1}{\sum_{i=0}^{v} e^{-(i-\mu_1)^2/2\delta_1^2}}$$

$$P_2 = \frac{N_2 \sigma_2}{\sum_{i=v}^{255} e^{-(i-\mu_2)^2/2\delta_2^2}}$$

A hill-climbing method is used to minimize $\sum_{i=0}^{255} [f(i) - F(i)]^2$.

4. The resultant best fitting *f(i)* is tested for bimodality based on some simple criteria.
5. Only for windows with bimodal fittings *f(i)* a threshold is selected that minimizes the probability of misclassification for the mixture distribution *f(i)*. This threshold *t* satisfies [4]

$$\left(\frac{1}{\sigma_1^2} - \frac{1}{\sigma_2^2}\right) t^2 + 2\left(\frac{\mu_2}{\sigma_2^2} - \frac{\mu_1}{\sigma_1^2}\right) t + \frac{\mu_1^2}{\sigma_1^2} - \frac{\mu_2^2}{\sigma_2^2} + 2\ln\frac{P_2\sigma_1}{P_1\sigma_2} = 0$$

6. Thresholds are then defined for the other windows by a local weighting averaging process. Let $T(u,v)$ be the threshold assigned to the window centered at (u,v) or 0 if no threshold was assigned to that window. Then for a window centered at (x,y) for which no threshold has yet been assigned, the threshold is computed with a mask:

$$\begin{bmatrix} \frac{\sqrt{2}}{2} & 1 & \frac{\sqrt{2}}{2} \\ 1 & x & 1 \\ \frac{\sqrt{2}}{2} & 1 & \frac{\sqrt{2}}{2} \end{bmatrix}$$

The resulting array of thresholds is smoothed using the array of weights:

$$\begin{bmatrix} \frac{\sqrt{2}}{2} & 1 & \frac{\sqrt{2}}{2} \\ 1 & 2 & 1 \\ \frac{\sqrt{2}}{2} & 1 & \frac{\sqrt{2}}{2} \end{bmatrix}$$

7. A threshold is assigned to individual pixels by bilinear interpolation on the window thresholds. Let P be surrounded by 4 windows A,B,C,D, where the thresholds for these windows are T_A, T_B, T_C, T_D respectively.

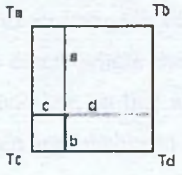

Fig. 8. Bilinear interpolation
Rys. 8. Interpolacja biliniowa

The threshold for P is taken as:

$$t = \frac{bdT_a + bcT_b + daT_c + caT_d}{(a+b)(c+d)}$$

If P is not surrouned by 4 window centers its threshold is taken to be that at the nearest window center.

Fig 9 shows the table of histograms, Fig 10 - the fitted bimodal histograms, while Fig 11 shows the result of the described local thresholding method.

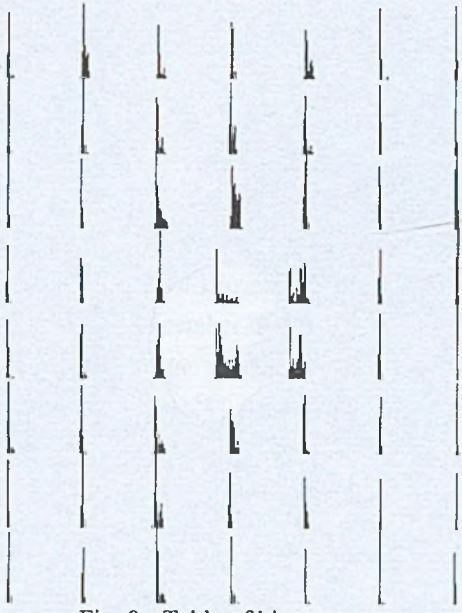

Fig. 9. Table of histograms
Rys. 9. Okna histogramów

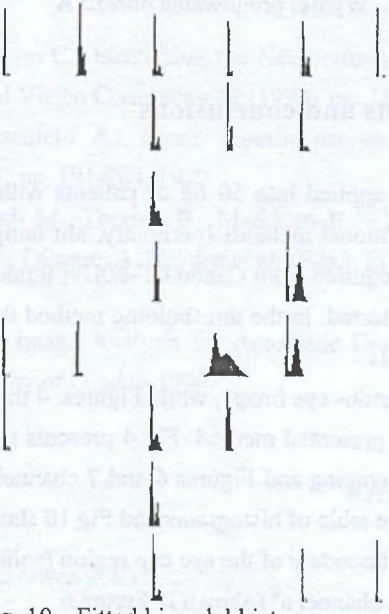

Fig. 10. Fitted bimodal histograms
Rys. 10. Dopasowane histogramy bimodalne

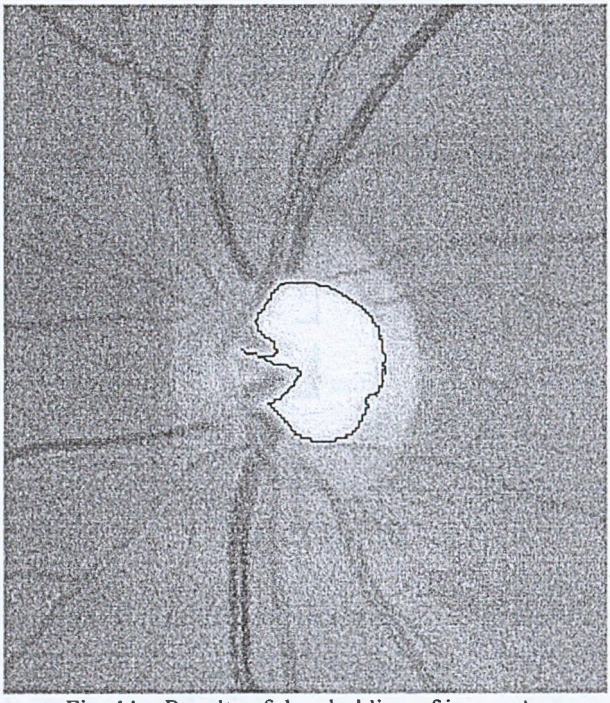

Fig. 11. Results of thresholding of image A
Rys. 11. Wyniki progowania obrazu A

3. Experimental results and conclusions

The new method has been applied into 50 fei of patients with glaucoma, which where previously examined by conventional methods (perimetry, slit lamp with Volk lens) and 50 fei of normal patients. On the acquired from Canon CF-60Uvi fundus camera images, the eye cup contour is automatically detected. In the thresholding method the image was divided into 56 windows each of 50x50 pixels.

Fig 3 shows the sampled fundus eye image, while Figures 4 through 11 show the results of the successive stages of the presented method. Fig 4 presents the detected blood vessels, Fig 5 the result after vessels averaging and Figures 6 and 7 channels a* and b* of the image shown in Fig 3. Fig 9 shows the table of histograms and Fig 10 shows the bimodal smoothed histograms. Fig 11 presents the boundary of the eye cup region (solid line) obtained as a result of thresholding the image (i.e. a channel a*) shown in Figure 6.

It is important to note that contours of the eye-cup obtained as a result of the presented segmentation method coincide with the contour marked by an ophthalmologist. The results of using the presented method are very encouraging.

The feature extraction of the suitable eye-cup shape descriptors as well as a classification of the segmented fundus eye images into normal and glaucomatous ones are now developed.

REFERENCES

1. Chaudhuri S., Chatterjee Sh., Katz N., Nelson M., Goldbaum M.: Detection of Blood Vessels in Retinal Images Using Two-Dimensional Matched Filter. IEEE Transactions on Medical Imaging, Vol 8, No. 3, September 1989.
2. Cheng H. D. et al.: Color image segmentation: advances and prospects. Pattern Recognition, Vol. 34, No 3, p. 2259-2281, 2001.
3. Goh K. G., et al: ADRIS: an Automatic Diabetic Retinal Image Screening system. K. J. Cios (Ed.): Medical Data Mining and Knowledge Discovery, pp 181-210, Springer-Verlag New York, November 2000.
4. Gonzalez R. C., Woods R. E.: Digital Image Processing. Prentice-Hall, 2002.
5. Jonas J.B., Budde W. M., Panda-Jonas S.: Ophthalmoscopic evaluation of the optic nerve head. Survey of Ophthalmology, Vol. 43, Nb. 4 January – February 1999
6. Kanski J. et al.: Glaucoma. A color manual of diagnosis and treatment. Butterworth-Heinemann, 1996.
7. Morris D.T., Donnison C.: Identifying the Neuroretinal Rim Boundary Using Dynamic Contours. Image and Vision Computing 17 (1999), pp. 169-174.
8. Nakagawa Y., Rosenfeld A.: Some experiments on variable thresholding. Pattern Recognition, vol. 11, pp. 191-204, 1979.
9. Osareh A., Mirmehdi M., Thomas B., Markham R.: Classification and Localisation of Diabetic-Related Eye Disease. A. Heyden et al. (Eds.): ECCV 2002, LNCS 2353, pp. 502-516, 2002
10. Sinthanayothin Ch.: Image Analysis for Automatic Diagnosis of Diabetic Retinopathy. Phd Thesis, University of London 1999.

Recenzent: Dr inż. Damian Bereska

Wpłynęło do Redakcji 9 czerwca 2003 r.

Omówienie

W artykule przedstawiono nowy algorytm automatycznej segmentacji wnęki naczyniowej na cyfrowych obrazach dna oka. Składa się on z następujących faz: (rys. 1): konwersje modeli kolorów, uśrednianie naczyń krwionośnych (rys. 5), opcjonalne poprawienie kontrastu i lokalne adaptacyjne progowanie (rys. 10). Kolejne etapy lokalnego progowania to: znalezienie tablicy lokalnych okien histogramu, dopasowanie bimodalnych histogramów, obliczenie lokalnych progów oraz stworzenie mapy progów bazując na procesie interpolacji biliniowej.

Znalezione zaproponowanym algorytmem segmentacji kontury wnęki naczyniowej pokrywają się z tymi, które wskazał lekarz okulista. Ekstrakcja cech wnęki jak i deskryptory kształtu oraz klasyfikacja segmentowanych obrazów na kategorie chorych i zdrowych są obecnie przedmiotem dalszych badań.

Adresy

Katarzyna STĄPOR: Politechnika Śląska, Instytut Informatyki, ul. Akademicka 16, 44-101 Gliwice, Polska, delta@ivp.iinf.polsl.gliwice.pl .
Lesław PAWLACZYK: Politechnika Śląska, Instytut Informatyki, ul. Akademicka 16, 44-101 Gliwice, Polska, palles@polsl.gliwice.pl .
Marek RZENDKOWSKI: Szpital Wielospecjalistyczny, Oddział Okulistyczny, ul. Kościuszki, 44-100 Gliwice, Polska.